

# Water Confined in Lamellar Structures of AOT Surfactants: An Infrared Investigation

C. Boissière,<sup>†</sup> J. B. Brubach,<sup>‡,§</sup> A. Mermet,<sup>‡,§</sup> G. de Marzi,<sup>‡</sup> C. Bourgaux,<sup>‡</sup> E. Prouzet,<sup>\*,†</sup> and P. Roy<sup>‡,§</sup>

*Institut Européen des Membranes, CNRS-UMR 5635, CNRS, 1919 Route de Mende, F-34293, Montpellier Cedex 5 (France), LURE, CNRS-UMR 130, Bat 209D, Université Paris-sud, F-91405 Orsay Cedex, (France), and CPMA, CNRS-UMR 8611, Bat. 490, Université Paris-sud, F-91405 Orsay Cedex, (France)*

*Received: July 16, 2001; In Final Form: November 5, 2001*

Both X-ray diffraction and infrared spectroscopy on water confined between the lamellar bilayers of aerosol-OT (AOT) allowed us to explore the differences in connectivity between bulk and confined water when water layer thicknesses are allowed to vary from 19.0 to 1.5 nm. Compared with previous studies on AOT reverse micelles, the present report in the lamellar mesophase allows one to cancel the micelle curvature contribution, which disrupts the water connectivity, too. The influence of AOT surface on the water connectivity degree was thus quantified alone in the mid infrared region (3000–3800 cm<sup>-1</sup>) in the OH stretching mode. The OH stretching mode peak can be fitted by three Gaussian peaks that describe three main connecting populations, namely the “multimer” water at c.a. 3585 cm<sup>-1</sup>, the “intermediary” water at c.a. 3465 cm<sup>-1</sup>, and the “network” water at c.a. 3320 cm<sup>-1</sup>. It is shown that interactions with the surfactant heads do not alter the water structure until the water layer shrinks below 4.0 nm and the hydration water molecules per surfactant are found to be equal to 2.6, in good agreement with equivalent studies on micellar systems.

## I. Introduction

Upon confining, fluids and especially liquids withstand drastic changes in their physical properties. These modifications are of great interest in several areas, such as material science, biology, or geology, all disciplines that deal with multicomponent systems.<sup>1,2</sup> Among various liquids, water is a highly correlated system by itself, where molecules withstand dynamic interactions through hydrogen bondings, which lead to the formation of large clusters and long-range water networks.<sup>3–11</sup> The intermolecular structure of water has been demonstrated to be modified near hydrophobic surfaces,<sup>12</sup> liquid crystals,<sup>13</sup> or in confined systems such as reverse micelles.<sup>14–23</sup> Water in oil (W/O) reverse micelle microemulsions, though simple models, allow a first step in the understanding of biological environments.<sup>21,22</sup>

In these systems, as in reverse micelles, both the local interaction with the hydrophilic surfactant headgroups and the geometry of the confining volume may modify the water connectivity characteristics. Although the case of reverse micelle systems has been widely investigated through infrared spectroscopy, equivalent studies for two-dimensional systems are still lacking. The interest for 2D systems lies in their simple geometry and may reveal a role played by the curvature in the modification of connectivity and the degree of hydration.

A surfactant such as aerosol OT (AOT, sodium di-2-ethylhexyl sulfosuccinate) offers a specific advantage for similar studies since it can lead to lamellar bilayers of the anionic surfactant in a wide range of AOT/water ratios, namely from 10 wt % to more than 60 wt %, between which water can be

confined to a controllable thickness. Modulating the water layer thickness should allow us to isolate or to evaluate the contribution of the surfactant surface on the degree of confinement disturbance of the water structure, without the disturbance coming from the micelle curvature. Comparison with similar AOT reverse micelle will then provide comparative information on the water structure in this two-dimensional confinement.

It has been shown that the OH stretching mode (3000–3800 cm<sup>-1</sup>) in the mid infrared region (MIR) is a good probe of the intermolecular water interactions because this contribution is sensitive to the nature of intermolecular bonding.<sup>14,15,19,21,22</sup> An accurate determination of the stretching modes, depending on the degree of connectivity for each water molecule, is obviously impossible, but simple models have shown to be useful tools for a quantitative evaluation of the extent of bonding of water molecules among each other and to the ionic headgroups. In this case, the mid-infrared band of the water network structure is roughly described by three levels of connectivity: a “network water” (NW) at c.a. 3320 cm<sup>-1</sup>, an “intermediate water” (IW) at c.a. 3465 cm<sup>-1</sup>, and a “multimer” water (MW) at c.a. 3585 cm<sup>-1</sup>, respectively.<sup>22,21</sup>

We report here a mid-infrared study of water trapped in lamellar systems whose thickness were varied between 1.0 and 20.0 nm. Unlike equivalent infrared studies on 3D micellar systems in which the main goal was to obtain the amount of affected water as a function of the total water content, our results are presented for sizable thickness determined by X-ray diffraction.

## II. Experimental Section

AOT (bis (2-ethylhexyl) sulfosuccinate sodium salt) from Fluka (98% grade) was used as received. Aqueous solutions of AOT were prepared with deionized water and AOT weight ratios of 5, 10, 20, 30, 40, 50, and 60 wt %. Samples were kept in

\* Corresponding author: E-mail: prouzet@iemm.univ-montp2.fr

<sup>†</sup> Institut Européen des Membranes.

<sup>‡</sup> LURE.

<sup>§</sup> CPMA.

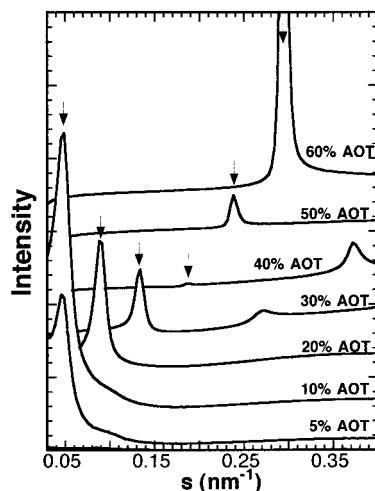


**Figure 1.** X-ray diffraction patterns of samples prepared with different weight ratios of AOT. The arrows indicate the position of the 001 diffraction peak.

sealed flasks and infrared spectra were recorded two months after their preparation. The water thickness of the different lamellar samples was determined from X-ray diffraction (XRD). The occurrence of lamellar structures was checked by optical polarized microscopy prior to the IR and diffraction experiments.

XRD experiments were conducted at the D24 beamline of the DCI synchrotron ring at LURE (Orsay, France). A Si(111) single-crystal curved monochromator provided a beam focused in the horizontal plane. The selected wavelength was 149 pm. The incident beam intensity was monitored by an ionization chamber and its size (typically  $0.4 \times 1.5 \text{ mm}^2$ ) was determined by collimating slits downstream from the monochromator. To reduce absorption and parasitic scattering, the beam path was kept under vacuum and slits were placed before the sample to suppress parasitic signal. The sample-to-detector distance was adjusted to 1.7 m in order to cover the required scattering vector range. The scattering patterns were recorded with a gas-filled, position sensitive detector. Samples were put in 1-mm thick cells sealed with Kapton windows. Three spectra of 600 s each were recorded symmetrically from the direct beam, then folded and averaged. The X-ray diffraction pattern was only corrected from the water filled cell background.

The mid-infrared transmission spectra were recorded using a Bomen DA8 Fourier transform spectrometer, at the SIRLOIN beamline of the SACO ring at LURE (Orsay, France).<sup>24,25</sup> This device can operate with an internal infrared source or with the infrared radiation emitted by the synchrotron ring. The mid-infrared region ( $500$  to  $9000 \text{ cm}^{-1}$ ) was recorded with a Globar source, in combination with a KBr beam splitter and a MCT wide-range detector. A specific cell (thickness  $\approx 75 \text{ }\mu\text{m}$ ) thermostated at  $20 \pm 0.2 \text{ }^\circ\text{C}$  was used with  $\text{CaF}_2$  windows. The spectra were recorded with a resolution of  $4 \text{ cm}^{-1}$  (100 scans per spectrum). No mathematical correction (e.g., smoothing) was done, and the spectra were corrected only from the empty cell contribution.

### III. Results and Discussion

**1. Diffraction Data.** X-ray diffraction patterns of the different samples are displayed in Figure 1 as a function of the wave vector  $s$  ( $s = 1/d = 2 \sin \theta/\lambda$ ). The AOT 5 wt % sample does not exhibit lamellar structure (it does not polarize light) but isotropic onion-like vesicles. The diffraction peak thus observed corresponds to the  $d$  spacing between different shells of the vesicle.

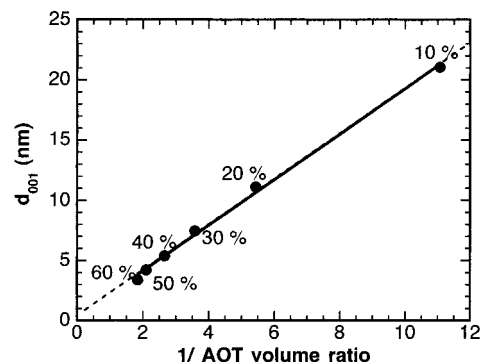


**Figure 2.** Evolution of the 001  $d$  spacing with the inverse of the AOT volume ratio.

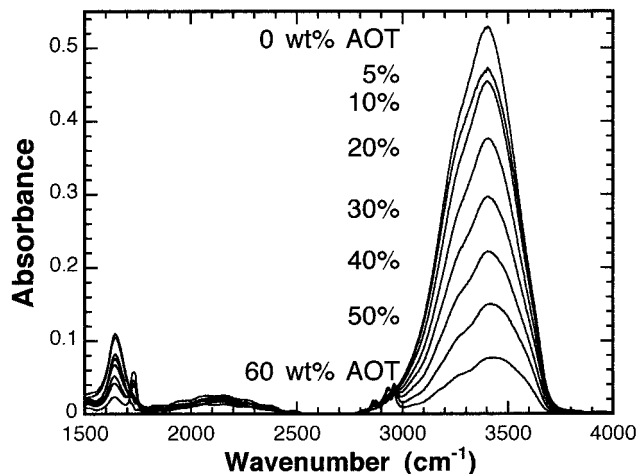


**Figure 3.** Mid-infrared spectra of samples prepared with different weight ratios of AOT.

The diffraction peaks observed for samples with AOT weight ratios ranging between 10% and 60% originate from the (001) diffracting planes of the lamellar structures. From the (001) peak position (see arrows in Figure 1), one can deduce the value of a  $d$  spacing, which includes the water thickness and the AOT bilayer thickness. The peak position is seen to decrease from  $4.7 \cdot 10^{-2} \text{ nm}^{-1}$  ( $d = 21.2 \text{ nm}$ ) down to  $29.4 \cdot 10^{-2} \text{ nm}^{-1}$  ( $d = 3.4 \text{ nm}$ ).

Figure 2 displays the evolution of the  $d$  spacing as a function of the inverse of the AOT volume ratio ( $\rho(\text{AOT}) = 1.1 \text{ g cm}^{-3}$ ). The observed linear dependence shows that  $d_{001} \text{ (nm)}$  is proportional to the water amount. A linear fit of these data leads to the following relationship:

$$d_{001} \propto 1.89/(\text{AOT volume ratio}) \quad (R = 0.9986) \quad (1)$$

The slope is assigned to the thickness of the “dried” membrane, which is the thickness of the AOT bilayer, in perfect agreement with previously reported values.<sup>26</sup> The value 1.9 nm corresponds to the length of two nonpenetrating AOT molecules. Therefore, the water thickness between two AOT bilayers is easily evaluated using the formula

$$\text{water thickness (nm)} = d_{001} - 1.9 \quad (2)$$

Thus, it appears that water lamellar structures can be obtained in the AOT system with thicknesses varying from 19.0 nm to c.a. 1.5 nm.

**2. Infrared Data.** Figure 3 displays the respective mid-IR spectra of different compositions, from pure water to the 60 wt % AOT sample. The less intense band at  $1650 \text{ cm}^{-1}$  corresponds

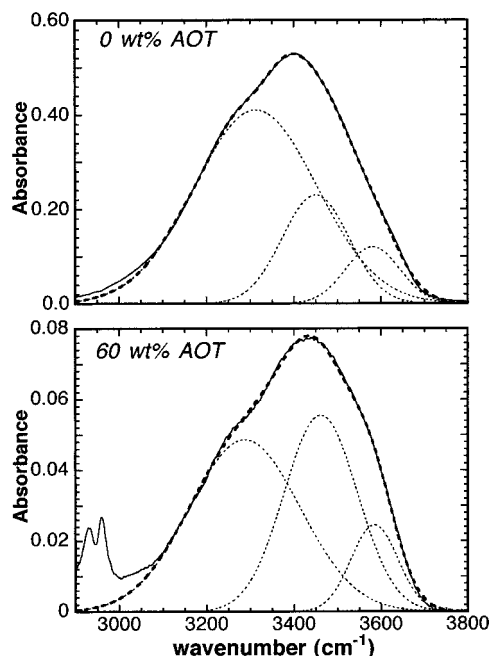


**Figure 4.** Comparison of the experimental curve (line) with the fitted one (bold dashed) obtained by the addition of the three single Gaussian functions (dashed), for the 0 wt % and 60 wt % AOT samples.

to the H<sub>2</sub>O bending mode (not studied herein). The total OH band area was found to increase linearly with increasing water content, and thus with increasing  $d_{001}$ .

For each concentration, the OH band was fitted using three Gaussian functions according to similar previous studies.<sup>14,15,19,21,22</sup> In bulk water, the three Gaussians are assumed to account for three dominating water “populations”, which differ from each other through their mean degree of connectivity. The low-energy Gaussian represents network water (NW) molecules that are bound to four other water molecules. Such species are most likely to be involved in extended transient water networks. The medium energy Gaussian stands for water molecules that establish, on average, three bonds with their neighboring counterparts (“intermediate water”, IW). The highest energy Gaussian is ascribed to water molecules that bind with two other molecules (“multimer water”, MW). Figure 4 illustrates such three-component fits with bulk water and the 60 AOT wt % sample. In the present system, in addition to water–water bondings, water may also establish hydrogen bonds with ionic headgroups (“hydration water”). As can be seen, confining of water into lamellar structures affects the relative proportions of the three subbands, which may reflect the increase of the relative proportion of hydration water. The overall change of the different Gaussian areas is displayed in Figure 5, as a function of the water layer thickness.

For water layer thickness between 19.0 and 4.0 nm, the three relative populations remain constant and very close to that of bulk water. While the multimer water contribution does not evolve over the whole range, the two other contributions turn out to be modified as the water layer thickness decreases below 4.0 nm: even though network water always dominates, its proportion decreases from 65% down to 51% as the water layer thickness decreases from 4.0 to 1.5 nm. Concomitantly, the intermediate water contribution increases, of the same amount, from 25% up to 39%. The fact that the relative area of the subband associated with the multimer water contribution remains unchanged suggests that the space between ionic heads does not favor the formation and trapping of smaller water aggregates.

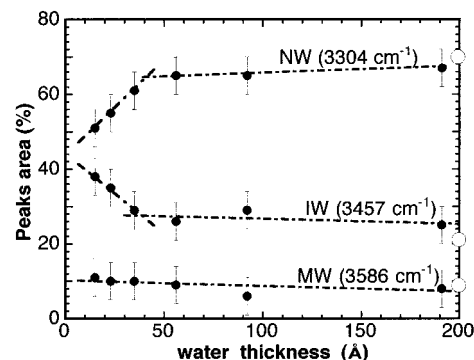


**Figure 5.** Evolution of the network water (NW), intermediary water (IW), and multimer water (MW) populations with the water thickness (open circles: pure water).

We interpret the relative population change as due to a growing proportion of hydration water molecules upon increasing confinement, since this population remains proportional to the number of surfactant headgroups at the interface, as is described below. Such molecules are likely to form a hydration layer, which acts as a buffer between the surfactant wall and the bulk-like inner part of the confined water layer.

The number of hydration molecules per surfactant molecule at the interface can be evaluated as follows. At a given water layer thickness  $T_{\text{layer}}$ , the evolving proportion  $P(\%) = \text{IW}(T_{\text{layer}}) - \text{IW}(T_{\text{layer}} \rightarrow 200 \text{ Å})$  accounts for the hydration water. The ratio of the hydration water layer volume to the total water layer volume is given by:

$$P = \frac{V_{\text{H}_2\text{O}}^{\text{hydration}}}{V_{\text{H}_2\text{O}}^{\text{total}}}$$

From there, one can estimate the number of water molecules per AOT headgroup at the interface. Let  $N_{\text{H}_2\text{O}}^{\text{hydration}}$  be the number of H<sub>2</sub>O molecules within the hydration layer and  $V_{\text{H}_2\text{O}}$  be the molecular volume of water (which, in a first approximation, we calculate from the volumetric mass of bulk water  $\rho = 1 \text{ g cm}^{-3}$ ). If  $N_{\text{AOT}}$  is the number of AOT molecules in contact with water, and  $S_{\text{AOT}}$  is the surface section of one AOT headgroup [ $S_{\text{AOT}} = 0.64 \text{ nm}^2$ ],<sup>27</sup> it follows:

$$N_{\text{H}_2\text{O}}^{\text{hydration}} V_{\text{H}_2\text{O}} = P \frac{N_{\text{AOT}} S_{\text{AOT}}}{2} T_{\text{layer}}$$

Therefore,

$$\frac{N_{\text{H}_2\text{O}}^{\text{hydration}}}{N_{\text{AOT}}} = P \frac{S_{\text{AOT}}}{2 v_{\text{H}_2\text{O}}} T_{\text{layer}}$$

Such evaluation can be reliably performed only for lamellar thicknesses smaller than  $\sim 4.0 \text{ nm}$ , that is as long as the Gaussian area values deviate significantly from those measured at large lamellar thickness (or in bulk water). One obtains a constant value for the hydration water molecules per surfactant of 2.6. This value is in very good agreement with that derived from equivalent studies on micellar studies.<sup>14</sup> It is remarkable that this same value was justified using thermodynamical approaches,<sup>14,15</sup> while in our case it is directly deduced from size measurements. As already noticed by Onori et al., “one can tentatively attribute the three binding sites on AOT molecules to the three oxygen atoms of the SO<sub>3</sub><sup>−</sup> headgroup to which water molecules could be hydrogen bonded”.

The constancy of 2.6 water molecules per ionic headgroup suggests that, in the range  $T_{\text{layer}} > 1.0$  nm, the hydration of the surfactant molecules is complete. This observation is supported by the fact that the position of the S=O stretching band ( $1045\text{ cm}^{-1}$ ) does not depend on the water layer thickness. This behavior is in contrast with micellar AOT systems, for which the S=O band position was seen to decrease upon increasing the micelle radius, until full hydration is reached.<sup>16,23</sup>

#### IV. Conclusion

The combined use of infrared spectroscopy and X-ray diffraction allowed us to quantitatively evaluate the extent of perturbation of water confined in lamellar systems. The investigation of the low water content region showed that, in these 2D systems, the characteristics of water confined between walls closer than 4.0 nm deviate from those of its bulky state, all the more so as the size is decreased. This deviation can be ascribed to the growing proportion of hydrating water molecules as the lamellar thickness is reduced. From the variation of the different water population and from size determination, the number of hydration water molecules per interface surfactant headgroup was found to be 2.6. This value is identical to that already observed with equivalent micellar 3D systems, at least in the case of large  $W$  values. Moreover, the space between ionic heads does not seem to enhance the formation and trapping of smaller water aggregates, as demonstrated by the constant value of the band attributed to multimer water.

Although mid-infrared measurements appear very adequate to the investigation of water confined in nanostructured liquids, the microscopic picture derived from our analysis relies from a rather indirect spectroscopic signature, namely the OH stretching band. Studies focusing on a more direct probe of the hydrogen bonding network, such as the so-called "connectivity" band arising around  $200\text{ cm}^{-1}$ , ascribed to the stretching motion of H-bonds,<sup>28,29</sup> should provide a less ambiguous description of these systems.

#### References and Notes

- (1) Israelachvili, J. N.; Gourdon, D. *Science* **2001**, 292, 867.
- (2) Heuberger, M.; Zäch, M.; Spencer, N. D. *Science* **2001**, 292, 905.

- (3) Stanley, H. E.; Teixeira, J. *J. Chem. Phys.* **1980**, 73, 3404.
- (4) Blumberg, R. L.; Stanley, H. E.; Geiger, A.; Mausbach, P. *J. Chem. Phys.* **1984**, 80, 5230.
- (5) Giguère, P. A. *J. Chem. Phys.* **1987**, 87, 4835.
- (6) Gerschel, A. *Liaisons Intermoléculaires*; InterEditions: Paris, 1995.
- (7) Guillaume, B. C. R.; Yoge, D.; Fendler, J. H. *J. Chem. Soc., Faraday Trans.* **1992**, 88, 1281.
- (8) Novaki, L. P.; El Seoud, O. A. *J. Colloid Interface Sci.* **1998**, 202, 391.
- (9) Ayotte, P.; Weddle, G. H.; Baley, C. G.; Johnson, M. A.; Vila, F.; Jordan, K. D. *J. Chem. Phys.* **1999**, 110, 6268.
- (10) Ayotte, P.; Weddle, G. H.; Johnson, M. A. *J. Chem. Phys.* **1999**, 110, 7129.
- (11) Devlin, J. P.; Joyce, C.; Buch, V. *J. Phys. Chem. A* **2000**, 104, 1974.
- (12) Scatena, L. F.; Brown, M. G.; Richmond, G. L. *Science* **2001**, 292, 908.
- (13) Calandra, P.; Caponetti, E.; Chillura Martino, D.; D'Angelo, P.; Minore, A.; Turco Liveri, V. *J. Mol. Struct.* **2000**, 522, 165.
- (14) Temsamani, M. B.; Maeck, M.; El Hassani, I.; Hurwitz, H. D. *J. Phys. Chem. B* **1998**, 102, 3335.
- (15) Onori, G.; Santucci, A. *J. Phys. Chem.* **1993**, 97, 5430.
- (16) Li, Q.; Weng, S.; Wu, J. *J. Phys. Chem. B* **2000**, 104, 9011.
- (17) Li, Q.; Li, T.; Wu, J.; Zhou, N. *J. Phys. Chem. B* **1998**, 102, 3168.
- (18) Fioretto, D.; Freda, M.; Mannaioli, S.; Onori, G.; Santucci, A. *J. Phys. Chem. B* **1999**, 103, 2631.
- (19) Jain, T. K.; Varshney, M.; Maitra, A. *J. Phys. Chem. B* **1989**, 93, 740.
- (20) MacDonald, H.; Bedwell, B.; Gulari, E. *Langmuir* **1986**, 2, 704.
- (21) Brubach, J.-B.; Mermet, A.; Filabozzi, A.; Colavita, P.; Gerschel, A.; Roy, P. *J. Phys. IV* **2000**, 10, Pr7/215.
- (22) Brubach, J.-B.; Mermet, A.; Filabozzi, A.; Colavita, P.; Gerschel, A.; Lairez, D.; Roy, P. *J. Phys. Chem. B* **2001**, 105, 430.
- (23) Moran, P. D.; Bowmaker, G. A.; Cooney, R. P. *Langmuir* **1995**, 11, 738.
- (24) Roy, P.; Mathis, Y.-L.; Gerschel, A.; Marx, J.-P.; Michaut, J.; Lagarde, B. *Nucl. Instrum. Methods Phys. Res.* **1993**, A325, 568.
- (25) Roy, P.; Mathis, Y.-L.; Lupi, S.; Tremblay, B.; Nucara, A.; Tadjeddine, A. *Ferroelectrics* **1996**, 176, 261.
- (26) Kotlarchyk, M.; Sheu, E. Y.; Capel, M. *Phys. Rev. A* **1992**, 46, 928.
- (27) Eastoe, J.; Towey, T. F.; Robinson, B. H.; Williams, J.; Heenan, R. K. *J. Phys. Chem.* **1993**, 97, 1453.
- (28) Hasted, J. B.; Husain, S. K.; Frescura, F. A. M.; Birch, J. R. *Chem. Phys. Lett.* **1985**, 118, 622.
- (29) Asfar, M. N.; Hasted, J. B. *J. Opt. Soc. Am.* **1977**, 67, 902.